Transactions of the TSME (2017) Vol. 5, No. 1, 65-73
Journal of Research and Applications in Mechanical Engineering

ISSN 2229-2152 print
DOI: 10.14456/jrame.2017.6

Research Article

NUMERICAL THERMAL PERFORMANCE ANALYSIS IN A HEAT EXCHANGER TUBE WITH V-SHAPED DISCRETE RIBS

S. Sripattanapipat*
S. Huyanan
Department of Mechanical Engineering, Faculty of Engineering, Mahanakorn University of Technology, 140 Chum Sampan Rd., Nong Chok, Bangkok, 10530, Thailand

ABSTRACT:
This paper presents a numerical investigation on thermal and flow behaviors in a heat exchanger tube fitted with three pairs of 45 deg. V-shaped discrete ribs (VDR) placed repeatedly along the tube wall. Air employed as the test fluid flows into the isothermal ribbed tube for Reynolds numbers (Re) between 3000 and 20,000. The finite volume method was applied for the computations whereas the SIMPLE algorithm was employed for handling the pressure-velocity coupling. This study shows that there are three pairs of counter-rotating vortices that can induce reattachment flows on the ribs and its vicinity resulting in greater increase in thermal performance. Moreover, influences of relative rib height (e/D) and pitch (PR=P/D) on heat transfer behaviors are reported. The investigation reveals that the increment of e/D results in the increasing rate of heat transfer and pressure loss while the rise of PR gives the reversing trend. The use of VDR yields very high thermal performance compared with the smooth tube.

Keywords: *Numerical analysis, Heat transfer, Discrete V-ribs, Turbulent flow*

1. INTRODUCTION

The need of high-efficiency heat exchanger devices paves the way to the development of heat transfer enhancement (HTE) techniques in designing those devices. Examples of the development include dimpled, grooved, corrugated and ribbed tubes apart from various tube inserts found in the literature for many years. For years, several ribs have been extensively used in many heat exchangers to increase the convection coefficients resulting in higher thermal performance of the systems. Webb [1] examined experimentally the effects of various rib parameters on thermal characteristics in a round tube with helical-ribs. Pal and Saha [2] reported heat transfer augmentation in a circular tube with combined spiral ribs and twisted tapes. Wang and Sunden [3] employed the liquid crystal technique (LCT) and PIV technique to investigate thermal behaviors in a channel fitted with discrete V-shaped ribs and indicated that the ribs provided considerably higher thermal performance. Li et al. [4] introduced the flow visualization by dying injection in a tube with double discrete inclined rib (DDIR-tube) and the appearance of multiple streamwise vortex flows in the DDIR-tube was visible. A numerical and experimental work was conducted by Tang et al. [5] to examine the pattern of flow and thermal characteristics in a channel with various discrete ribs placed on the principal walls. Kathait and Patil [6] investigated experimentally the flow friction and thermal behaviors in a corrugated tube with gaps. A numerical simulation of the tube flow model with sixteen rib shapes was performed by Moon et al. [7] who suggested that the best thermal performance was for the new boot-shaped rib where its pressure loss was the same as that for the square rib.

* Corresponding author: S. Sripattanapipat
E-mail address: ssomchai@mut.ac.th

Xie et al. [8] studied numerically an effect of the truncated ribs having serveral offset placements and angles on flow and thermal characteristics in a square duct and found that the best overall thermal performance was for 45° inclined mid-truncated ribs. Wang et al. [9] numerically and experimentally examined thermal characteristics of turbulent channel flow through ribs, to find out the compromise between the rate of heat transfer and the enlarged pressure loss. From the studies above, the application of ribs can assist to increase the rate of heat transfer in a round tube with a certain extent of friction loss. Therefore, the numerical simulation of a three-dimensional turbulent tube flow through the 45° V-shaped discrete rib (VDR) is conducted with the key purpose being to investigate the change of flow structure and thermal behaviors.

2. TUBE FLOW CONFIGURATION

A flow model of interest is characterized by three VDR pairs mounted repeatedly around a circular tube surface as displayed in Fig. 1 below. The model in the current work is expected to attain a periodically fully-developed flow where the velocity field repeats itself from one module to another. This concept of the periodically fully developed flow and it solution procedure was initially introduced by Patankar et al. [10]. In the model, air flows into the VDR tube having the inner diameter, D=20 mm at inlet temperature (T_{in}) of 300 K. The rib parameters are the single rib width (W=1.0 mm) and the attack angle (α=45°). e and P stand for rib height and pitch while the varied e/D and PR=P/D are in the range of 0.03-0.05 and 0.5-1.0, respectively.

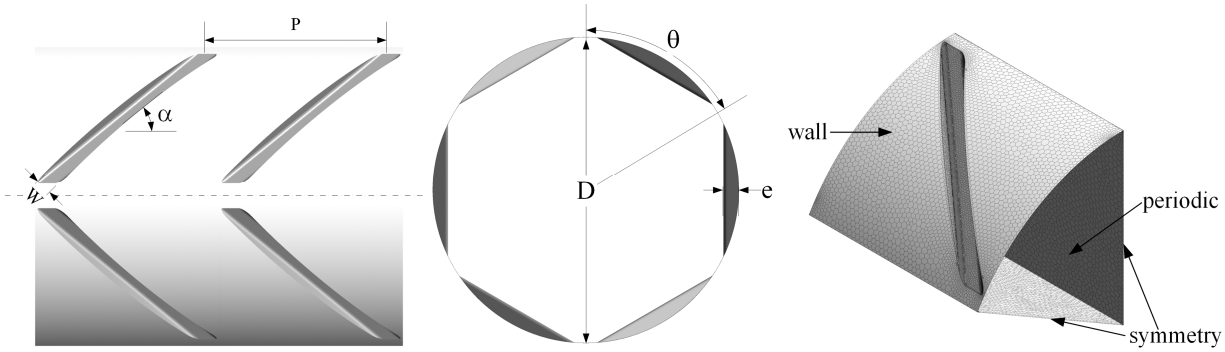

Fig. 1. Tube geometry and computational domain.

3. COMPUTATIONAL DETAILS

The numerical flow model for investigating the flow pattern and thermal characteristics in the VDR tube is under the assumptions as follows:

- Steady three-dimensional turbulent flow.
- Constant fluid properties.
- Body forces, viscous dissipation and radiation heat transfer are omitted.

As above, the Reynolds averaged Navier-Stokes (RANS) equations and the energy equation are applied. Those equations can be written as:
Continuity equation:

$$\frac{\partial}{\partial x_i}\left(\rho u_i\right) = 0 \tag{1}$$

Momentum equation:

$$\frac{\partial}{\partial x_j}\left(\rho u_i u_i\right) = -\frac{\partial p}{\partial x_i} + \frac{\partial}{\partial x_j}\left[\mu\left(\frac{\partial u_i}{\partial x_j} + \frac{\partial u_j}{\partial x_i}\right) - \rho\overline{u_i' u_j'}\right] \tag{2}$$

in which ρ, u_i, p, μ and u' are density, mean velocity component in direction x_i, pressure, dynamic viscosity, and fluctuating velocity component, respectively. Repeated indices mean summation of one to three for 3D problems.

Energy equation:

$$\frac{\partial}{\partial x_j}\left(\rho u_i T\right)=\frac{\partial}{\partial x_j}\left(\left(\Gamma+\Gamma_t\right)\frac{\partial T}{\partial x_j}\right) \tag{3}$$

where Γ and Γ_t are molecular thermal diffusivity and turbulent thermal diffusivity, respectively and are given by

$$\Gamma=\frac{\mu}{\mathrm{Pr}}, \text{ and } \Gamma_t=\frac{\mu_t}{\mathrm{Pr}_t} \tag{4}$$

The Reynolds stress terms, $-\rho\overline{u_i'u_j'}$ appearing in Eq. (2) needs to be modeled. These Reynolds stresses are related to the mean velocity gradients using Boussinesq hypothesis as can be seen in the equation below:

$$-\rho\overline{u_i'u_j'}=\mu_t\left(\frac{\partial u_i}{\partial u_j}+\frac{\partial u_j}{\partial u_i}\right)-\frac{2}{3}\left(\rho k+\mu_t\frac{\partial u_i}{\partial x_i}\right)\delta_{ij} \tag{5}$$

in which k and δ_{ij} are turbulent kinetic energy, defined by $k=1/2\cdot\overline{u_i'u_i'}$ and a Kronecker delta. The application of Boussinesq approach is because of very low computational cost in computing the turbulent viscosity, μ_t defined as $\mu_t=\rho C_\mu k^2/\varepsilon$. As a result, the Boussinesq hypothesis is included in the RNG k–ε model.

The transport equations of k and ε are expressed as:

$$\frac{\partial}{\partial x_i}\left(\rho k u_i\right)=\frac{\partial}{\partial x_j}\left(\alpha_k\mu_{eff}\frac{\partial k}{\partial x_j}\right)+G_k-\rho\varepsilon \tag{6}$$

$$\frac{\partial}{\partial x_i}\left(\rho\varepsilon u_i\right)=\frac{\partial}{\partial x_j}\left(\alpha_\varepsilon\mu_{eff}\frac{\partial\varepsilon}{\partial x_j}\right)+C_{1\varepsilon}\frac{\varepsilon}{k}G_k-C_{2\varepsilon}\rho\frac{\varepsilon^2}{k}-R_\varepsilon \tag{7}$$

As above, α_k and α_ε are, respectively, the inverse effective Prandtl number for k and ε while $C_{1\varepsilon}$ and $C_{2\varepsilon}$ are constants.

The effective viscosity μ_{eff} is written by

$$\mu_{eff}=\mu+\mu_t=\mu+\rho C_\mu\frac{k^2}{\varepsilon} \tag{8}$$

where C_μ is a constant and set to 0.0845, derived using the ‘‘renormalization group” (RNG) method.

The QUICK numerical scheme was employed for discretizing all the governing equations whereas the SIMPLE algorithm was used for pressure-velocity coupling before being solved by a finite volume approach [11]. The RNG k-ε model was utilized for closure of the equations. No slip and constant temperature for rib surfaces and tube walls were set for boundary conditions. The periodic flow condition was applied to the entry and exit sections from the fully-developed periodic flow assumption while the one-sixth tube section was used due to axis symmetry as shown in Fig. 1. The solution was considered to be converged for the residual values of all variables less than 10^{-6} except for the energy equation less than 10^{-9}. Details on grid independence test and other conditions are the same as the baffled duct in [12].

Four parameters of interest in the current work are Reynolds number (Re), friction factor (*f*), Nusselt number (Nu) and thermal enhancement factor (TEF).

The Re is defined as

$$\mathrm{Re}=\frac{\rho\bar{u}D}{\mu} \tag{9}$$

The f is evaluated from pressure drop, Δp across the tube length, L as

$$f = \frac{(\Delta p / L)D}{(1/2)\rho \bar{u}^2} \tag{10}$$

The local Nu is calculated by

$$Nu_x = \frac{h_x D}{\lambda} \tag{11}$$

where λ is fluid thermal conductivity.
The area-averaged Nu is obtained from

$$Nu = \frac{1}{A}\int Nu_x \partial A \tag{12}$$

TEF is defined as the ratio of dimensionless convection coefficient of the ribbed tube, Nu to that of the smooth tube, Nu_0, at similar blowing power and is given by

$$TEF = \frac{Nu / Nu_0}{(f / f_0)^{1/3}} \tag{13}$$

in which Nu_0 and f_0 are for smooth tube only, respectively.

4. RESULTS AND DISCUSSION

4.1 Validation

The verification of the numerical with experimental results of a round tube with double discrete ribs [13] is shown in Fig. 2a and b for Nu and f, respectively. The numerical results are in good agreement with experimental data for both Nu and f. The maximum deviations for both results are about 5% for Nu and 15% for f. Thus, the numerical model in the current study is judged to be reliable.

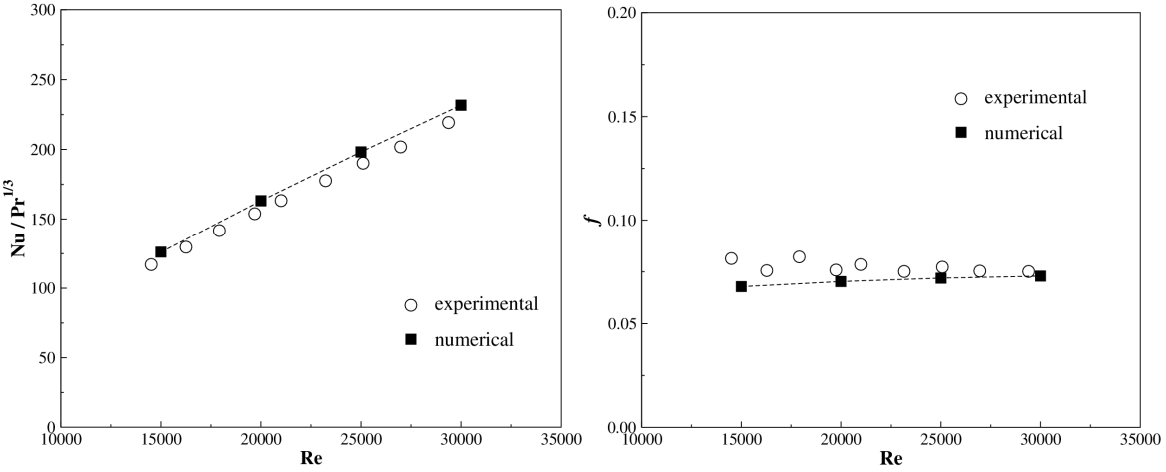

(a) (b)

Fig. 2. Validation of (a) Nu and (b) f with measurement.

4.2 Flow structure

Fig. 3a, b and c exhibits respectively the plots of velocity vectors, streamlines, and temperature contours on transverse planes for e/D=0.05, PR=0.5 and Re=12,000. As seen in the figure, three counter-rotating vortices appear

around the tube cross section (see Fig. 3b). The appearance of three pairs of counter-rotating vortices leads to the considerable heat transfer augmentation in the tube.

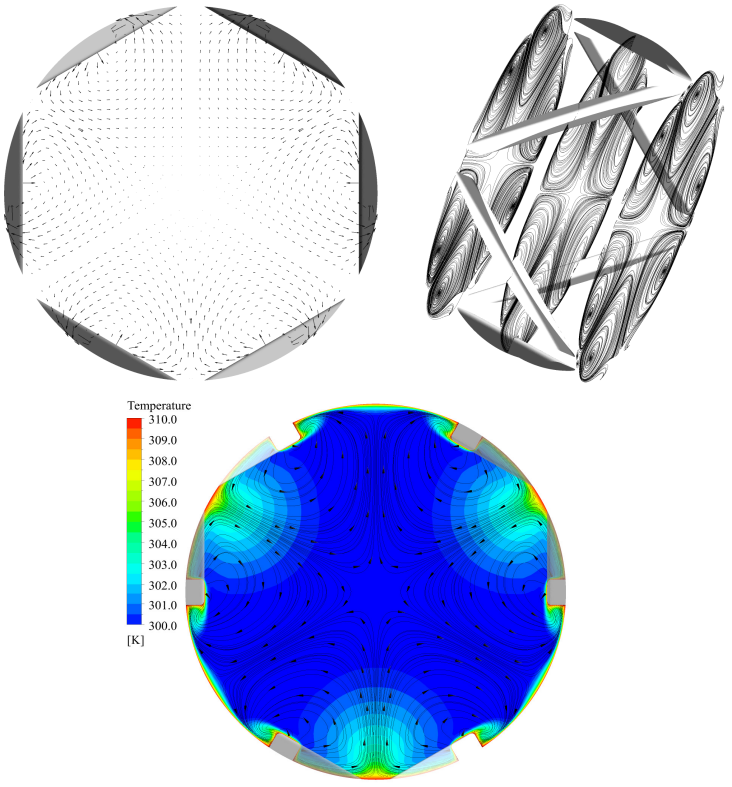

(a) (b) (c)

Fig. 3. (a) Velocity vectors, (b) streamlines and (c) temperature contours on transverse plane, for e/D=0.05, PR=0.5 and Re=12,000.

The plot of temperature contours is for the VDR tube with e/D=0.05 and PR=0.5 at Re=12,000 as displayed in Fig. 3c. The temperature field is changed dramatically due to three pairs of vortices. The higher temperature gradients are found for three regions where the velocity flows toward the surface or common-flow-down vortices, while the lower ones are for the regions where the velocity flows away from the wall surface due to common-flow-up vortices.

Fig. 4a shows streamlines in the vicinity of the VDR. There are two vortices appearing around the rib element: front vortex appearing in the front of the rib and the rear vortex behind the rib. The rear vortex is stronger and larger and has a significant effect on the heat transfer rate.

To visualize the vortices in the 3D flow, a detecting method of the coherent structure based on the Q-criterion is offered. A rotation structure is raised to visualize them as an "iso-surface" of a constant Q, where $Q > 0$ is realized. The center direction of vortex flow is displayed by viewing the iso-surface of $Q/Q_{max} = 0.01$ as seen in Fig. 4b. It is observed in the figure that the vortex core seen downstream of the rib leading end, moves across the rib cavity to the trailing end of the downstream rib before merging the upstream vortex core and then repeats itself. The appearance of three main counter-rotating vortices leads to flow impingement and higher vortex strength.

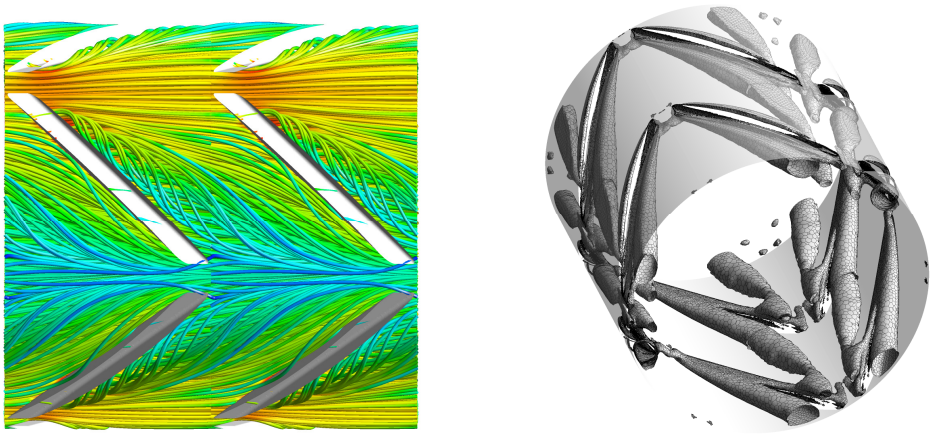

(a) (b)

Fig. 4. (a) streamlines around VDR and (b) iso-surfaces of Q/Q_{max}=0.01 for e/D=0.05, PR=0.5 and Re=12,000.

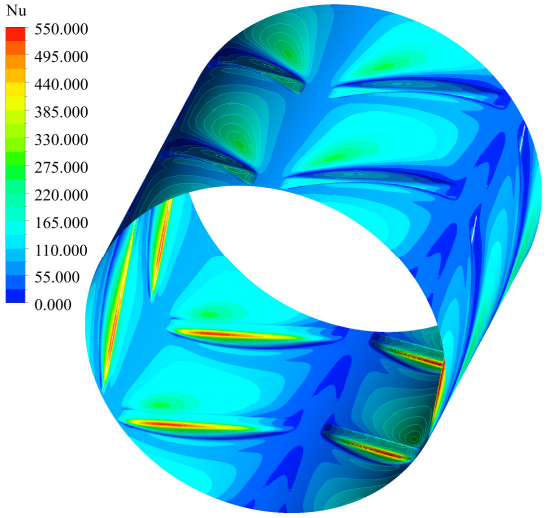

Fig. 5. Local Nu contours on rib and tube surfaces, e/D=0.05, PR=0.5, Re=12,000.

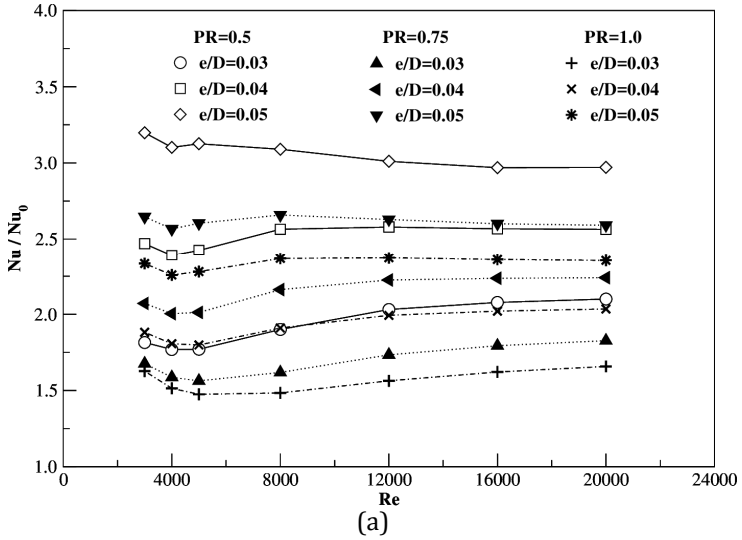

(a)

Fig. 6. Variations of (a) Nu/Nu_0, (b) f/f_0 and (c) TEF with Re.

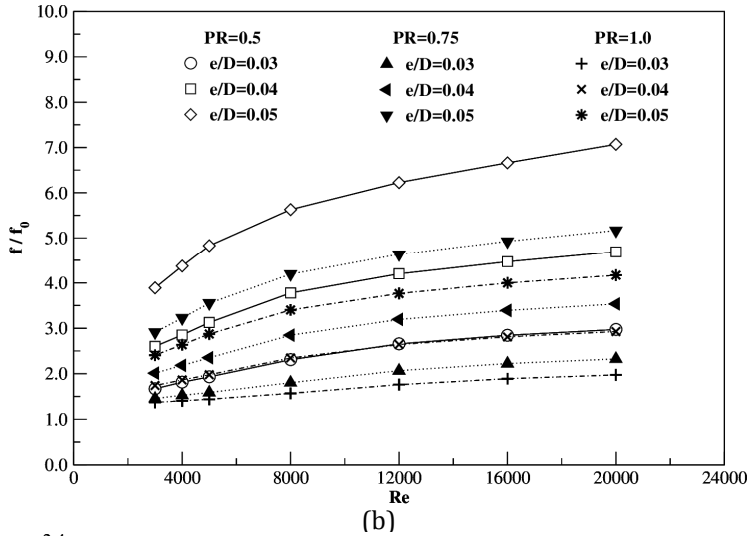

Fig. 6. Variations of (a) Nu/Nu_0, (b) f/f_0 and (c) TEF with Re. (*continued*)

4.3 Heat transfer

Fig. 6a depicts the distributions of Nu/Nu_0 with Re for using the VDR at different e/D and PR. In the figure, Nu/Nu_0 displays the downtrend at the beginning with the increase of Re until Re > 6000 before showing the slightly increasing trend for further Re. Nu/Nu_0 also has the uptrend with increasing e/D while shows the reversing trend for increasing PR. The maximum Nu/Nu_0 value is around 3.23 at e/D=0.05, PR=0.5 and Re=3000.

4.4 Friction loss

The HTE is involved with pressure loss in the form of increased *f*. Fig. 6b displays the distributions of f/f_0 with Re for using the VDR elements at different PR and e/D values. It is visible that f/f_0 tends to increase with the increment in e/D but shows the downtrend with increasing PR. At e/D = 0.05, the highest f/f_0 is around 7.0 at PR=0.5 and Re=20,000.

4.5 Thermal performance

Fig. 6c shows the variation of TEF with e/D and PR for various Re values. In the figure, TEF tends to decrease with the rise in PR and Re while displays the opposite trend for e/D. It is found that the VDR tube with e/D = 0.05 and PR=0.5 yields the highest TEF of 2.04 at Re=3000. The TEF is found to be in the range of 1.22 to 2.04.

5. CONCLUSION

A numerical study on turbulent flow and thermal characteristics in the discrete V-ribbed tube has been conducted. The use of the VDR elements leads to the appearance of three pairs of counter-rotating vortices that is the key reason for heat transfer enhancement in the tube. The HTE in the tube with VDRs is around 1.4 to 3.23 times higher than the smooth tube alone while the friction factor is enlarged in a range of 1.17 to 7.0 times. TEF of the VDR tube is above unity and has a maximum of about 2.05 at PR=0.5 and e/D=0.05. This indicates this VDR tube is a promising technique for HTE of tubular heat exchanger systems.

NOMENCLATURE

A	heat transfer surface area, m^2
D	inner diameter of tube, m
e	rib height, m
f	friction factor
h	convective heat transfer coefficient, W/m^2-K
k	turbulent kinetic energy, J/kg
L	length of test section, m
Nu	Nusselt number
P	axial pitch spacing of rib, m
PR	relative rib pitch ratio (P/D)
ΔP	pressure drop, Pa
Pr	Prandtl number
Re	Reynolds number
T	temperature, K
TEF	thermal enhancement factor
W	rib width, m
Greek Letters	
α	attack angle of rib, degree
θ	sector angle of rib, degree
ρ	fluid density, kg/m^3
v	kinematic viscosity, m^2/s
λ	fluid thermal conductivity, W/m-K
ε	dissipation rate, J/kg-s
Subscripts	
a	air
i, j	index
max	maximum
o	smooth tube
t	turbulent

REFERENCES

[1] Webb, R., Narayanamurthy, R., and Thors, P. Heat transfer and friction characteristics of internal helical-rib roughness, J. Heat Transf., Vol. 122, 2000, pp. 134-142.

[2] Pal, S. and Saha, S.K. Laminar fluid flow and heat transfer through a circular tube having spiral ribs and twisted tapes, Exp. Therm. Fluid Sci., Vol. 60, 2015, pp. 173-181.

[3] Wang, L. and Sunden, B. An experimental investigation of heat transfer and fluid flow in a rectangular duct with broken V-shaped ribs, Exp. Heat. Transf., vol. 17, 2004, pp. 243-259.

[4] Li, X.W.,Yan, H., Meng, J.A. and Li, Z.X. Visualization of longitudinal vortex flow in an enhanced heat transfer tube, Exp. Therm. Fluid Sci., Vol. 31, 2007, pp. 601-608.

[5] Tang, X.Y. and Zhu, D.S. Flow structure and heat transfer in a narrow rectangular channel with different discrete rib arrays, Chem. Eng. Process., Vol. 69, 2013, pp. 1-14.

[6] Kathait, P.S. and Patil, A.K. Thermo-hydraulic performance of a heat exchanger tube with discrete corrugations, Appl. Therm. Eng., Vol. 66, 2014, pp. 162-170.

[7] Moon, M.A., Park, M.J. and Kim, K.Y. Evaluation of heat transfer performances of various rib shapes, Int. J. Heat Mass Transf., Vol. 71, 2014, pp. 275-284.
[8] Xie, G., Liu, J., Ligrani, P.M. and Sunden, B. Flow structure and heat transfer in a square passage with offset mid-truncated ribs, Int. J. Heat Mass Transf., Vol. 71, 2014, pp. 44-56.
[9] Wang, H., Lee, W., Chan, J. and To, S. Numerical and experimental analysis of heat transfer in turbulent flow channels with two-dimensional ribs, Appl. Therm. Eng., Vol. 66, 2014, pp. 162-170.
[10] Patankar, S.V., Liu, C.H. and Sparrow, E.M. Fully developed flow and heat transfer in ducts having streamwise-periodic variations of cross-sectional area, ASME J. Heat Transf., Vol. 99, 1977, pp. 180-186.
[11] Versteeg, H.K. and Malalasekera, W. An Introduction to Computational Fluid Dynamics: The Finite Volume Method, Longman Scientific & Technical, Longman Group Limited, 1995.
[12] Promvonge, P., Changcharoen, W., Kwankaomeng, S. and Thianpong, C. Numerical heat transfer study of turbulent square-duct flow through inline V-shaped discrete ribs, Int. Commun. Heat Mass Transf., Vol. 38, 2011, pp. 1392-1399.
[13] Li, X.W., Meng, J.A. and Guo, Z.Y. Turbulent flow and heat transfer in discrete double inclined ribs tube, Int. J. Heat and Mass Transf., Vol. 52, 2009, pp. 962-970.